Kinetics of Metallocarbohedrenes: An FT-ICR Mass Spectrometry Study of the Association Reactions of $Ti_8C_{12}^+$ with Polar and Nonpolar Molecules

Ken J. Auberry,* Yong Gwan Byun, Denley B. Jacobson, and Ben S. Freiser†

H. C. Brown Laboratory of Chemistry, Purdue University, West Lafayette, Indiana 47907

Received: June 3, 1999

The reactivity of the metallocarbohedrene cluster $Ti_8C_{12}^+$ is studied by Fourier transform ion cyclotron resonance (FT-ICR) mass spectrometry. Rate constants for the addition of various polar molecules (NH_3, H_2O, and CH_3CN) and nonpolar molecules (C_2H_4 and C_6H_6) to $Ti_8C_{12}^+$ are determined by isolating each $Ti_8C_{12}(L)_x^+$ (L = NH_3, H_2O, CH_3CN, C_6H_6, or C_2H_4) species and monitoring the decay of the parent ion as a function of time. For NH_3 and H_2O, four fast additions are observed, with additional associations occurring at a greatly reduced rate, while reactions of $Ti_8C_{12}(CH_3CN)_x^+$ ($x = 0-4$) with CH_3CN come to a complete halt after the association of the fourth molecule of CH_3CN. We propose that ligand polarity plays a key role in the dramatic decrease in rate constant observed for addition reactions which occur after the attachment of a fourth polar molecule to the cluster.

Introduction

Metallocarbohedrenes, or met-cars, were discovered by Castleman and co-workers in 1992.[1−4] These compounds, with the general formula M_8C_{12} (M = early transition metal), appear as unusually intense peaks in the mass spectra of clusters generated by a laser-desorption-powered molecular cluster ion source in which a He expansion gas is seeded with a hydrocarbon. These clusters have been extensively studied by both theoretical and experimental means in order to better understand structure/reactivity relationships.[5−23] Originally, a pentagonal dodecahedral structure with T_h symmetry was proposed by Castleman and co-workers.[1−5] However, distorted structures such as tetracapped tetrahedra with T_d or D_{2d} symmetries have been predicted to be thermodynamically more stable in some cases.[13−23] For example, Rohmer et al. have estimated that the T_d and D_{2d} structures of $Ti_8C_{12}^+$ are, respectively, 190 and 154 kcal/mol more stable than the T_h structure.[22]

The absence of macroscale quantities of these clusters prevents their study by physical methods such as X-ray diffraction or spectroscopic techniques that could probe their structures. Consequently, other methodologies involving ion mobility and ion−molecule reactivities have been employed to probe the structure of met-cars.[5−12] Recently, Bowers and co-workers have shown evidence that $Ti_8C_{12}^+$ exists as a hollow cage structure by using innovative ion mobility measurements. While these experiments readily ruled out the more unusual cubic structures suggested by Khan[21] and Pauling,[24] they could not unequivocally distinguish between structures having T_h and T_d symmetries.[11] Reactivity studies carried out by Castleman and co-workers considered the manner and magnitude with which neutral molecules attach to $Ti_8C_{12}^+$.[5,12] These experiments were carried out in the relatively high reagent pressure source (approximately 0.7 Torr) of a triple-quadrupole instrument. They observed the attachment of eight small polar molecules (such as H_2O, NH_3, methanol, and 2-butanol) that occur rapidly and with no observable break in the product distribution. Polar and nonpolar molecules with π-bonding systems (such as acetonitrile, benzene, and ethene) were shown to give four attachments, again with no observable break in the product distribution. The disparity between the bonding of these two different types of molecules was explained through the interactions of the π-systems of these molecules with the metal−metal bond between two titanium centers in the pentagonal rings of the T_h structure.[12] These observations are consistent with a pentagonal dodecahedral structure having T_h symmetry. However, recent experimental evidence presented by Freiser and co-workers has examined the relative addition kinetics for $V_8C_{12}^+$ and $Nb_8C_{12}^+$ species.[8−10] These results reveal a pattern of four rapid additions of small polar molecules followed by four much slower additions, with a distinct break in the product distribution after the fourth addition.

Here, we report the first systematic study of the kinetics of adduct formation for the reactions of simple molecules with $Ti_8C_{12}^+$. Our results reveal appreciable differences in the addition kinetics for $Ti_8C_{12}L_n^+$ (L = adduct molecule). Typically, the addition kinetics become progressively slower as additional molecules are added; however, a dramatic decrease in the rate constant is observed for the addition of a fifth neutral molecule to $Ti_8C_{12}L_4^+$. These kinetic results may contribute to a better understanding of both the structure of the $Ti_8C_{12}^+$ cluster and its reactivity.

Experimental Section

All experiments were performed on an Extrel FTMS-2000 dual-cell FT-ICR mass spectrometer (Finnigan MAT, GmbH, Bremen, Germany),[25,26] equipped with a 3 T superconducting magnet and a compact supersonic source of the type developed by Smalley and co-workers.[27] A pure titanium target was vaporized by using the second harmonic of a pulsed Nd:YAG laser (532 nm) in a manner similar to that of Castleman and co-workers.[3,28] The metal plasma generated by the laser pulse was then reacted with a high-pressure, short-duration burst of a gas mixture from a fast pulsed valve (R. M. Jordan Company, Grass Valley, CA). This gas mixture consisted of approximately 5% CH_4 to provide a ready source of carbon for formation of the clusters, with the remaining 95% as helium to assist in

† Deceased December, 1997.

10.1021/jp991806s CCC: $18.00
Published on Web 10/21/1999

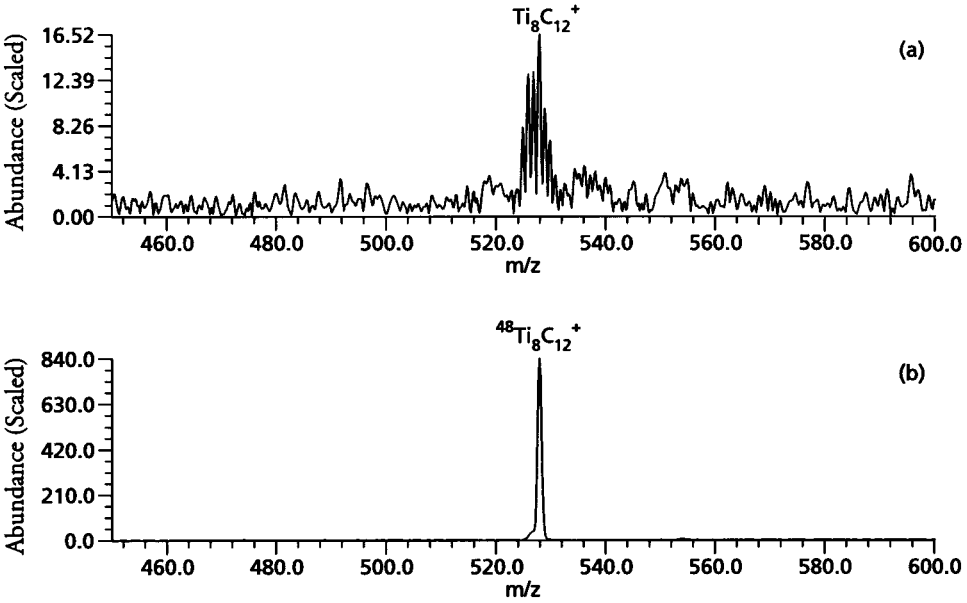

Figure 1. Spectra that show the effect of selected ion accumulation on the isolation of $Ti_8C_{12}^+$. (a) Signal with no quadrupolar axialization during the accumulation event. (b) Greater than 50× improvement in signal magnitude resulting from QEA.

expansive cooling of the newly formed clusters. Neutral reagents were introduced into the vacuum chamber at a low static pressure (10^{-8}−10^{-6} Torr) through Varian leak valves[29] with argon as the collision gas at a static pressure of $\sim 3.0 \times 10^{-6}$ Torr. Pressures were monitored by a calibrated Bayard-Alpert type ionization gauge. For rate constant measurements, reagent pressures in the cell were also corrected for ionization sensitivities.[30] These pressure measurements have an error of less than 30% and are the dominant factor in errors associated with the reaction rate constants. Consequently, reaction rate constants are assigned errors of ±30%.

Mass selection and ion isolation were accomplished by a combination of selected ion accumulation, described below, SWIFT,[31] and standard FT-ICR radio frequency pulses of variable frequency and power. Our instrument is outfitted with a quadrupolar excitation axialization (QEA) switching box, described in detail elsewhere.[32,33] QEA allows ions of a given mass-to-charge ratio to have their orbital radii constricted to the center of the trapping cell. Selected ion accumulation[34] works by irradiating the cell with radio frequency energy in the axialization mode at a frequency corresponding to the desired *m*/*z* ratio to be retained during the time that ions are being injected into the cell by the external cluster source. With this method, it is possible to trap a cluster of given *m*/*z* ratio with greatly increased efficacy by compressing it to the center of the trapping field while the remainder of the ions continue to expand out to the walls of the cell to be neutralized and pumped away. This technique requires a relatively high pressure of a neutral collision gas to provide the necessary damping needed to collapse the cyclotron orbits of the ions back to the center of the cell. This condition is easily met by the additional transient helium gas load from the expansive cooling of the clusters floods into the trapping cell, briefly increasing the pressure to $\sim 10^{-5}$ Torr. For the experiments described here, signal-to-noise ratio increases of 1−2 orders of magnitude were commonly seen when compared to otherwise identical spectra obtained without QEA. Figure 1 illustrates the dramatic, 50× improvement in signal magnitude achieved by using QEA during the accumulation of clusters from the external source.

Kinetic measurements were performed by isolating the individual reactant ions, $Ti_8C_{12}(L)_n^+$ ($n = 0$−5), after an initial product formation delay ranging from 0 to 10 s. These isolated ions were then allowed to react with a static background pressure of the neutral reagent for a variable time, in the presence of $\sim 3.0 \times 10^{-6}$ Torr argon. For example, to obtain kinetics for the addition of NH_3 to $Ti_8C_{12}(NH_3)_2^+$, the $Ti_8C_{12}^+$ cluster ion was first isolated and then allowed to react with NH_3 until sufficient abundance of $Ti_8C_{12}(NH_3)_2^+$ had been generated (1−10 s). The resulting $Ti_8C_{12}(NH_3)_2^+$ ion was then isolated and allowed to further react with NH_3. The high reagent pressures that would be required to observe multiple additions for very slow reactions ($> 1.0 \times 10^{-6}$ Torr) caused dramatic reductions in both the initial cluster signal and the length of time that ions can effectively be trapped. Consequently, reactions with relatively slow kinetics could not be studied.

Results

NH_3 Addition Kinetics. Ammonia reacts with $Ti_8C_{12}^+$ to yield simple sequential additions, as shown in Figure 2. These spectra indicate relatively rapid addition of four ammonia molecules to yield $Ti_8C_{12}(NH_3)_4^+$, with higher order species such as $Ti_8C_{12}(NH_3)_5^+$ and $Ti_8C_{12}(NH_3)_6^+$ slowly growing in abundance as the reaction time is increased to 20 s. Consequently, the rate constants for the addition of ammonia to $Ti_8C_{12}(NH_3)_n^+$ ($n = 0$−4) were carefully measured. The kinetic plots are illustrated in Figure 3 and clearly show that pseudo-first-order kinetics are observed for each addition.

The decay slopes from the pseudo-first-order kinetic plots of $Ti_8C_{12}(NH_3)_n^+$ ($n = 0$−4) with NH_3 are utilized in conjunction with the corrected ammonia pressure in the cell to obtain observed reaction rate constants, k_{obs}, for the addition of NH_3 to the cluster. Reaction efficiencies are calculated by comparing k_{obs} to the collision rate constants (average dipole orientation, k_{ADO} [35,36]) for each addition reaction. The data are summarized in Table 1. The relative rate constants for each subsequent ammonia addition are reduced by about 20% until the fifth addition, where there is a dramatic 83% reduction in the rate constant. The addition of a sixth ammonia was too slow to be measured, indicating a rate constant of $< 1.0 \times 10^{-12}$ cm^3 molecule^{-1} s^{-1}.

H_2O Addition Kinetics. H_2O reacts with $Ti_8C_{12}^+$ to yield simple, sequential adducts similar to those observed for the

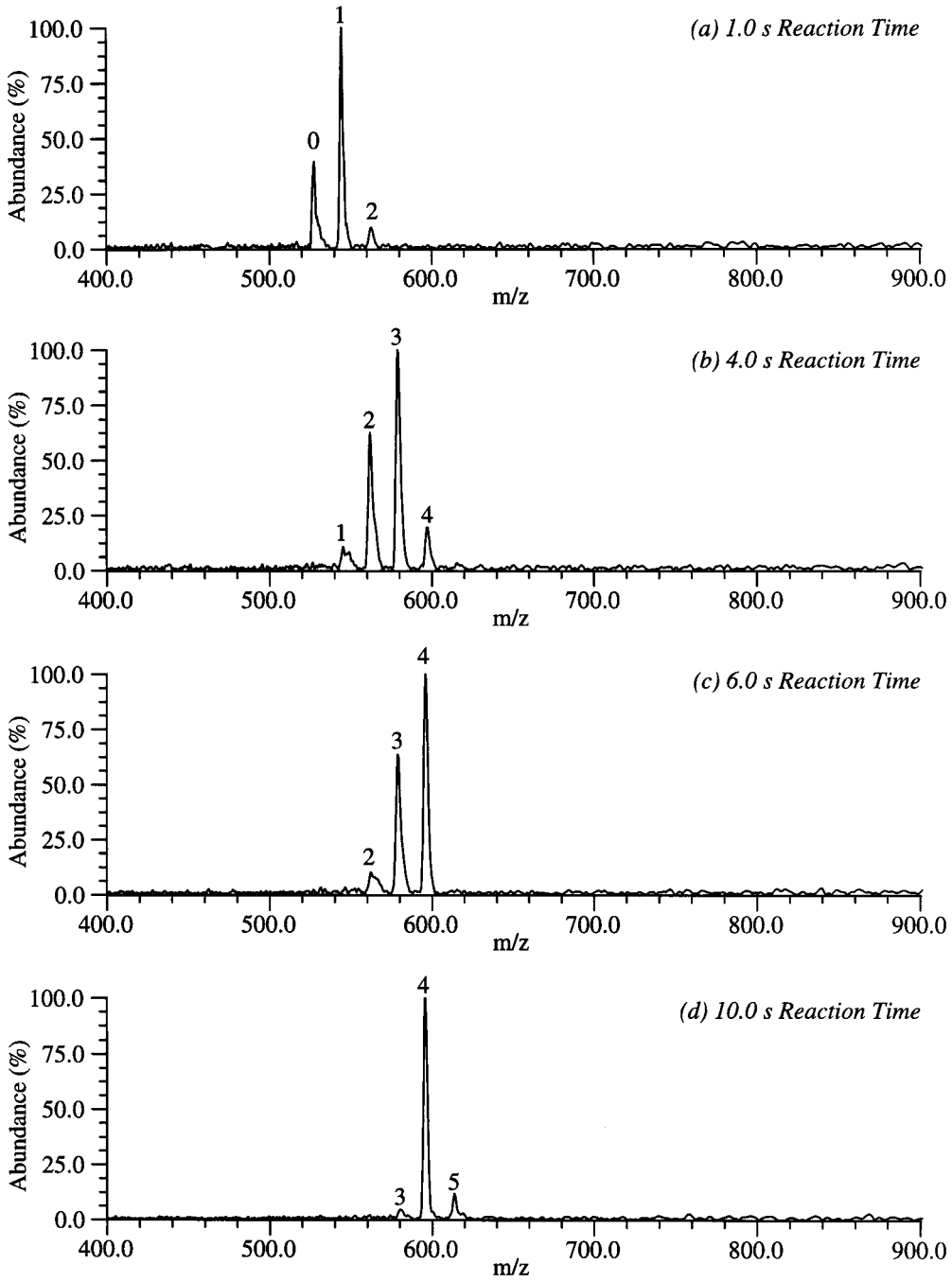

Figure 2. Reaction of $Ti_8C_{12}^+$ with NH_3 ($\sim 4.3 \times 10^{-8}$ Torr). Peak labels represent the number of NH_3 ligands attached to $Ti_8C_{12}^+$ at various reaction times: (a) 1 s; (b) 4 s; (c) 6 s; (d) 10 s.

ammonia reactions. This simple adduct formation is in contrast to the more complicated chemistry observed for $V_8C_{12}^+$ and $Nb_8C_{12}^+$, where dehydrogenations giving rise to hydroxyl species were observed.[8−10] The kinetic measurements were carried out as described above, with each addition peak individually isolated and reacted. The kinetic plots are illustrated in Figure 4 and again show simple pseudo-first-order kinetics. Reaction rate constants and efficiencies are summarized in Table 2.

A close examination of the kinetics indicates three rough groupings of rate constants. The first two additions proceed at approximately 60% of the collision rate, with the next three occurring at roughly 36% of the collision rate, or nearly half the rate of the first two additions. The sixth addition, however, proceeds at approximately 10% of the collision rate. Additional ligand associations up to $Ti_8C_{12}(H_2O)_7^+$ are observed, with an apparent product buildup at the seventh addition. However, due to insufficient signal magnitude, kinetic data for the seventh and eighth additions could not be obtained.

CH_3CN Addition Kinetics. CH_3CN reacts with $Ti_8C_{12}^+$ to yield simple attachment products similar to those discussed above. However, the product distribution seen for these reactions truncates sharply at $Ti_8C_{12}(CH_3CN)_4^+$, with no other higher order products observed. The rate constants for each of these reactions were measured in the same manner as above, with each addition peak individually isolated and reacted. Pseudo-first-order kinetics are observed for each of these reactions (see Figure 5). Reaction rate constants and efficiencies are summarized in Table 3.

Examination of the kinetic data indicates that the first two additions proceed at approximately the same rate (~50% efficiency), with the remaining two additions occurring at less

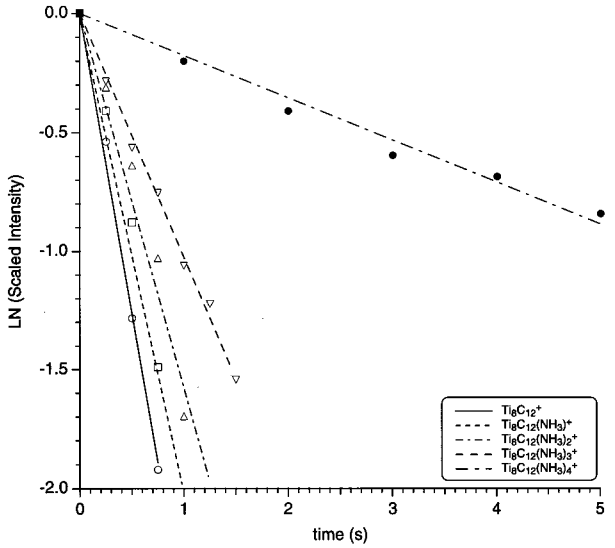

Figure 3. Combined kinetic plot for the addition reactions of $Ti_8C_{12}(NH_3)_n^+$ ($n = 0-4$) with NH_3. The data represent decay slopes of the reactant ions for each NH_3 addition. Kinetic data are summarized in Table 1.

TABLE 1: Measured Rate Constants for the Sequential Addition Reactions of $Ti_8C_{12}(NH_3)_n^+$ ($n = 0-4$) with NH_3[a]

reactant ion	k_{obs} (cm^3/s)	k_{ADO} (cm^3/s)	reaction efficiency	relative efficiency
$Ti_8C_{12}^+$	7.8×10^{-10}	1.6×10^{-9}	0.49	1.00
$Ti_8C_{12}(NH_3)^+$	6.3×10^{-10}	1.6×10^{-9}	0.39	0.81
$Ti_8C_{12}(NH_3)_2^+$	5.0×10^{-10}	1.6×10^{-9}	0.31	0.65
$Ti_8C_{12}(NH_3)_3^+$	3.0×10^{-10}	1.6×10^{-9}	0.19	0.38
$Ti_8C_{12}(NH_3)_4^+$	5.1×10^{-11}	1.6×10^{-9}	0.03	0.06

[a] NH_3 was present at a pressure of 1.0×10^{-7} Torr with Ar as the buffer gas at a pressure of $\sim 3.0 \times 10^{-6}$ Torr.

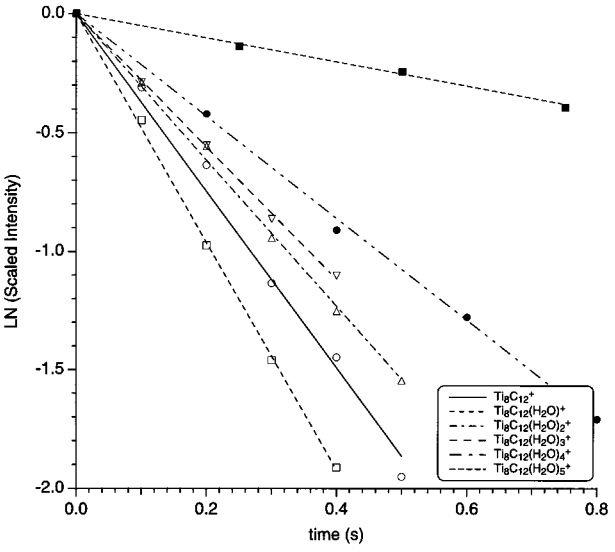

Figure 4. Combined kinetic plot for the addition reactions of $Ti_8C_{12}(H_2O)_n^+$ ($n = 0-4$) with H_2O. The data represent decay slopes of the reactant ions for each H_2O addition. Kinetic data are summarized in Table 2.

than half of that rate (~20% efficiency). No additional associations beyond $Ti_8C_{12}(CH_3CN)_4^+$ were observed, even at extended reaction times.

C_6H_6 Addition Kinetics. Benzene reacts with $Ti_8C_{12}^+$ to yield the same type of simple attachment products as seen for CH_3CN, with a product distribution that also sharply truncates at four ligand additions. No higher order products were observed

TABLE 2: Measured Rate Constants for the Sequential Addition Reactions of $Ti_8C_{12}(H_2O)_n^+$ ($n = 0-6$) with H_2O[a]

reactant ion	k_{obs} (cm^3/s)	k_{ADO} (cm^3/s)	reaction efficiency	relative efficiency
$Ti_8C_{12}^+$	8.4×10^{-10}	1.5×10^{-9}	0.56	1.00
$Ti_8C_{12}(H_2O)^+$	9.9×10^{-10}	1.5×10^{-9}	0.66	1.18
$Ti_8C_{12}(H_2O)_2^+$	6.4×10^{-10}	1.5×10^{-9}	0.43	0.76
$Ti_8C_{12}(H_2O)_3^+$	5.7×10^{-10}	1.5×10^{-9}	0.38	0.68
$Ti_8C_{12}(H_2O)_4^+$	4.6×10^{-10}	1.5×10^{-9}	0.31	0.55
$Ti_8C_{12}(H_2O)_5^+$	1.5×10^{-10}	1.5×10^{-9}	0.10	0.13

[a] H_2O was present at a pressure of 1.4×10^{-7} Torr with Ar as the buffer gas at a pressure of $\sim 3.0 \times 10^{-6}$ Torr.

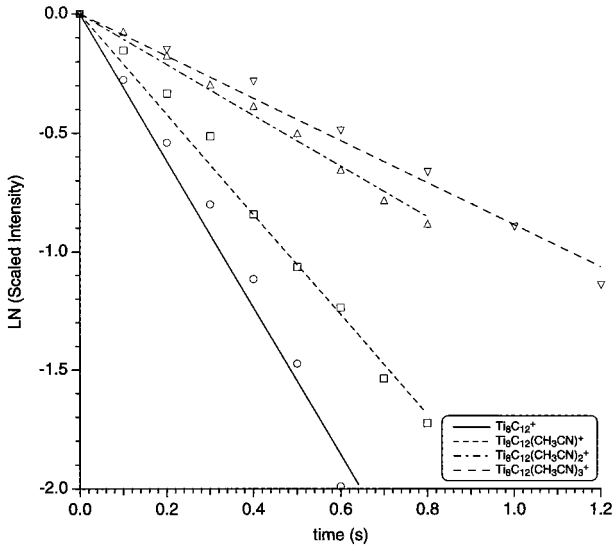

Figure 5. Combined kinetic plot for the addition reactions of $Ti_8C_{12}(CH_3CN)_n^+$ ($n = 0-4$) with CH_3CN. The data represent decay slopes of the reactant ions for each CH_3CN addition. Kinetic data are summarized in Table 3.

TABLE 3: Measured Rate Constants for the Sequential Addition Reactions of $Ti_8C_{12}(CH_3CN)_n^+$ ($n = 0-4$) with CH_3CN[a]

reactant ion	k_{obs} (cm^3/s)	k_{ADO} (cm^3/s)	reaction efficiency	relative efficiency
$Ti_8C_{12}^+$	1.4×10^{-9}	2.5×10^{-9}	0.58	1.00
$Ti_8C_{12}(CH_3CN)^+$	1.0×10^{-9}	2.5×10^{-9}	0.40	0.69
$Ti_8C_{12}(CH_3CN)_2^+$	5.7×10^{-10}	2.5×10^{-9}	0.23	0.40
$Ti_8C_{12}(CH_3CN)_3^+$	4.3×10^{-10}	2.5×10^{-9}	0.17	0.30

[a] CH_3CN was present at a pressure of 7.0×10^{-8} Torr with Ar as the buffer gas at a pressure of $\sim 3.0 \times 10^{-6}$ Torr.

at extended reaction times. Rate constants for each addition reaction were determined in the same manner as above, with each peak individually isolated and reacted. Pseudo-first-order kinetics were observed in all four cases, as shown in Figure 6. Rate constants and efficiencies for the reactions are summarized in Table 4.

C_2H_4 Addition Kinetics. $Ti_8C_{12}^+$ reacts with ethene to produce simple attachment products that appear to terminate at $Ti_8C_{12}(C_2H_4)_3^+$. These additions are very slow, occurring at 1% of the collision rate, necessitating the use of high pressures ($\sim 8.4 \times 10^{-7}$ Torr) of ethene to obtain any observable additions. By this same token, any associations occurring after the third addition were too slow to be measured. The rate constant for the addition of a fourth ethene was too small ($k < 1.0 \times 10^{-12}$ cm^3 $molecule^{-1}$ s^{-1}) to be measured. There does, however, appear to be a sharp drop-off that occurs in the reaction rate after the third addition, suggesting that subsequent associations would occur at a rate $< 1.0 \times 10^{-12}$ cm^3 $molecule^{-1}$ s^{-1}. Pseudo-

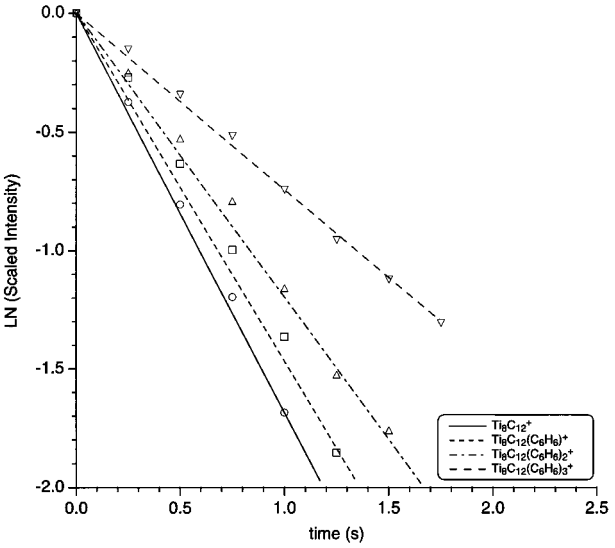

Figure 6. Combined kinetic plot for the addition reactions of $Ti_8C_{12}(C_6H_6)_n^+$ ($n = 0-4$) with C_6H_6. The data represent decay slopes of the reactant ions for each C_6H_6 addition. Kinetic data are summarized in Table 4.

TABLE 4: Measured Rate Constants for the Sequential Addition Reactions of $Ti_8C_{12}(C_6H_6)_n^+$ ($n = 0-4$) with C_6H_6[a]

reactant ion	k_{obs} (cm^3/s)	k_{ADO} (cm^3/s)	reaction efficiency	relative efficiency
$Ti_8C_{12}^+$	9.9×10^{-10}	9.2×10^{-10}	1.07	1.00
$Ti_8C_{12}(C_6H_6)^+$	8.9×10^{-10}	9.1×10^{-10}	0.98	0.90
$Ti_8C_{12}(C_6H_6)_2^+$	7.2×10^{-10}	9.0×10^{-10}	0.80	0.73
$Ti_8C_{12}(C_6H_6)_3^+$	4.4×10^{-10}	9.0×10^{-10}	0.49	0.45

[a] C_6H_6 was present at a pressure of 5.4×10^{-8} Torr with Ar as the buffer gas at a pressure of $\sim 3.0 \times 10^{-6}$ Torr.

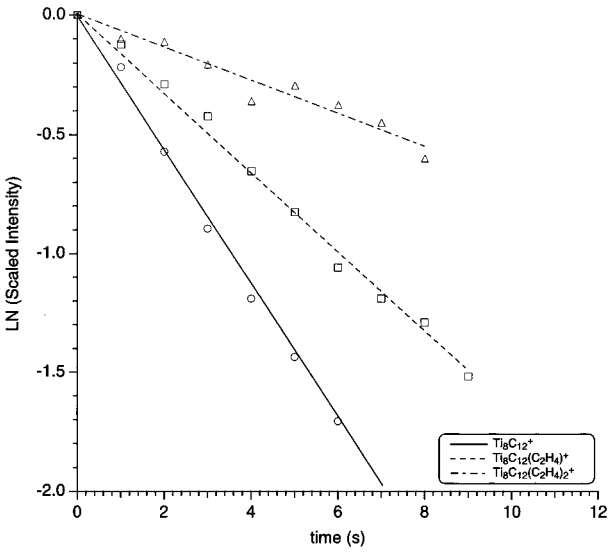

Figure 7. Combined kinetic plot for the addition reactions of $Ti_8C_{12}(C_2H_4)_n^+$ ($n = 0-3$) with C_2H_4. The data represent decay slopes of the reactant ions for each C_2H_4 addition. Kinetic data are summarized in Table 5.

first-order kinetics were observed in all cases, Figure 7. Rate constants and efficiencies for each reaction are summarized in Table 5.

Discussion

Reactions with Polar Molecules (H_2O, NH_3, and CH_3CN). The attachment of small polar molecules such as NH_3, H_2O, and CH_3CN to $Ti_8C_{12}^+$ clusters involves coordinative interactions between their lone-pair electrons and the empty orbitals of the individual metal centers. Thus, the attachment of up to eight ligands to the cluster is possible. However, both the number of ligands that can bind to the cluster and the corresponding rate constants for those attachments can be a sensitive function of stereoelectronic effects.

TABLE 5: Measured Rate Constants for the Sequential Addition Reactions of $Ti_8C_{12}(C_2H_4)_n^+$ ($n = 0-3$) with C_2H_4[a]

reactant ion	k_{obs} (cm^3/s)	k_{ADO} (cm^3/s)	reaction efficiency	relative efficiency
$Ti_8C_{12}^+$	1.0×10^{-11}	9.4×10^{-10}	0.011	1.00
$Ti_8C_{12}(C_2H_4)^+$	6.3×10^{-12}	9.4×10^{-10}	0.007	0.62
$Ti_8C_{12}(C_2H_4)_2^+$	1.2×10^{-12}	9.4×10^{-10}	0.001	0.12

[a] C_2H_4 was present at a pressure of 8.4×10^{-7} Torr with Ar as the buffer gas at a pressure of $\sim 3.0 \times 10^{-6}$ Torr.

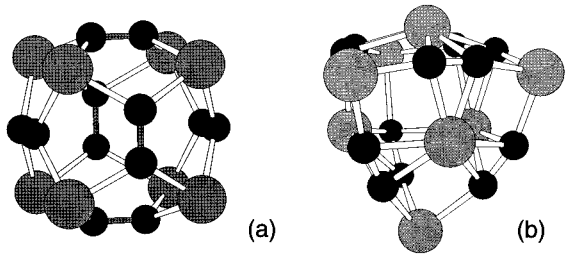

Figure 8. Cartoon representations of (a) the proposed T_h structure and (b) proposed T_d structure for the $Ti_8C_{12}^+$ cluster.

In a previous set of experiments, Castleman and co-workers reported the addition of up to eight molecules for reactions with H_2O, NH_3, CH_3OH, and 2-butanol with $Ti_8C_{12}^+$.[5,12] These results provide strong support for the T_h symmetric structure with eight equivalent metal sites (Figure 8a). However, they observed the addition of only four ligands for CH_3CN and pyridine. Our results, however, show a significant reduction in the rate constants after the addition of the fifth ligand for H_2O and fourth ligand for NH_3 (Figure 2). This result indicates that there is a dramatic change in the reactivity of the cluster at this point. In the case of CH_3CN, we only observe four rapid additions to the cluster.

The conditions under which the reactivity of these clusters is studied are quite different between the two groups. Reactions of the cluster in Castleman's work involved a high-pressure (approximately 0.7 Torr) reaction cell, allowing for the excess energy of the collision complex to be dissipated by stabilizing collisions with the He buffer gas. This results in rapid ligand additions to the cluster. In our work, the reactivity of the cluster was studied at a much lower buffer gas pressure ($\sim 3 \times 10^{-6}$ Torr) where stabilizing collisions with the buffer gas are unlikely. Under these low-pressure conditions, the only stabilization pathway available to the collision complex is infrared radiative emission. The probability of this type of stabilization is strongly dependent on the energy of attraction (i.e., binding energy) of the ion/molecule collision complex and scales almost linearly with the internal energy contained in the excited state complex.[37] Consequently, our results suggest that the binding energies for the sixth ligand for H_2O and the fifth ligand for NH_3 are measurably lower than that for the preceding ligand. In addition, the binding energy of a fifth ligand for CH_3CN, acetone, and pyridine must be much lower than that of the fourth ligand.

We now need to address why the binding energy of the fifth ligand is significantly weaker than that of the fourth ligand. All of the above molecules are highly polar, and the electronic

structure of the cluster is obviously affected by the association of additional ligands. Also, steric crowding is increased upon coordination of additional ligands. However, the interplay of steric and electronic effects is clearly a complex issue.

In a cluster with T_d symmetry (Figure 8b), there are two sets of four equivalent metal atoms with one set more reactive than the other. The "outer" set of metal atoms are σ-bonded to three C_2 subunits, with the metal and carbon atoms forming a tetrahedral skeleton for the cluster. The "inner" set of metal atoms are located on the faces of the tetrahedral skeleton and are coordinated through the π-systems of the C_2 subunits. Presumably, the "outer" set of metal atoms would be more reactive than the "inner" set. In this scenario, our results can be explained by these two sets of metal atoms with different reactivities.

However, our results can also be explained in terms of the T_h symmetry cluster with eight equivalent metal atoms. Here, the ligands may first coordinate to nonadjacent metal atoms, of which there are four. At this point, the fifth ligand must add to a metal atom where the three adjacent metal atoms are already coordinated. Although the metal is still sterically accessible, the three adjacent ligands may sufficiently hinder the accessibility to affect the kinetics. In addition, the electronic structure of the open metal site may also be changed due to an increase in electron density in the cluster. Consequently, our kinetic results simply do not provide compelling evidence as to the structure of the $Ti_8C_{12}^+$ cluster.

In comparing H_2O to NH_3, there is a less dramatic effect in going from the fourth to the fifth addition for H_2O. This may be due to hydrogen bonding between adjacent water molecules. This could slightly increase the overall binding energy of the fifth H_2O molecule. In the case of NH_3, the lone electron pair is not available for hydrogen bonding.

With CH_3CN, both our results and Castleman's show only the addition of four ligands. We clearly see the rapid addition of four ligands; consequently, there is a dramatic change for the addition of a fifth ligand. In addition, Castleman and co-workers reported the addition of only four molecules for acetone and pyridine. Castleman explains the addition of only four of these molecules by suggesting that they coordinate to the cluster through the π-system, bridging across two metal atoms.[12] Consequently, the coordination of four CH_3CN molecules ties up all of the coordination sites. These molecules, however, typically coordinate to transition metals and their clusters in an end-on fashion through the lone electron pair on the heteroatom (N or O). We believe that this is their mode of interaction with the $Ti_8C_{12}^+$ cluster. However, it is possible for the coordinated molecule to bend toward an adjacent open metal center so that the π-system can interact with that metal. Hence, coordination of four molecules would then tie up the eight metal sites.

We believe that all of the above polar molecules interact with the cluster in a similar manner, namely through coordination of the heteroatom to a Ti atom in the cluster. How can we explain the difference in reactivity of these molecules with the cluster? For pyridine, the explanation for the addition of only four molecules is probably due to steric bulk; only four pyridine molecules can coordinate to the cluster. However, for acetone and CH_3CN, steric crowding seems unlikely in light of the coordination of eight molecules of 2-butanol.[12] Although these molecules are all small and highly polar, CH_3CN and acetone are significantly more polar (Table 6). Theory predicts that the Ti atoms carry a large (+0.66 to +1.07) positive charge.[14,20] Therefore, there should be a strong attraction between the partially positive Ti atoms in the cluster and the partially negative ends of the polar molecules through electrostatic attraction. This electrostatic attraction should, however, be strongest for the highly polar CH_3CN and acetone molecules; yet, only four attachments are observed for these molecules. The initial attachment of four polar molecules would most likely involve coordination to nonadjacent Ti atoms in the cluster complex, an arrangement which would minimize repulsive forces between coordinated molecules. However, the fifth molecule would be required to approach a Ti atom for which the three adjacent Ti atoms are already occupied by attached molecules. The electrostatic repulsive force felt by the incoming molecule as it approaches the partially positive ends of these adjacent polar molecules should increase with polarity (Figure 9a). Consequently, the highly polar CH_3CN and acetone molecules should experience a higher repulsive force as these molecules approach the cluster. The electrostatic attraction between the partially negative heteroatom and the positive Ti atom would not become significant until the molecule was very close to the metal atom (Figure 9b). As a result, a fifth CH_3CN or acetone molecule simply cannot overcome the repulsive electrostatic barrier to form a stable complex. For H_2O and NH_3, this repulsive force should also play a similar role; however, it is only enough to greatly slow the addition of a fifth molecule, but not great enough to completely prevent it as was the case with both CH_3CN and acetone. In a future work we hope to investigate this theory further through the use of computer modeling techniques.

TABLE 6: Dipole Moments of Some Simple Molecules

molecule	dipole moment[38] (d)
NH_3	1.47
H_2O	1.85
CH_3OH	1.70
2-butanol	1.64
acetone	2.88
CH_3CN	3.92
pyridine	2.19

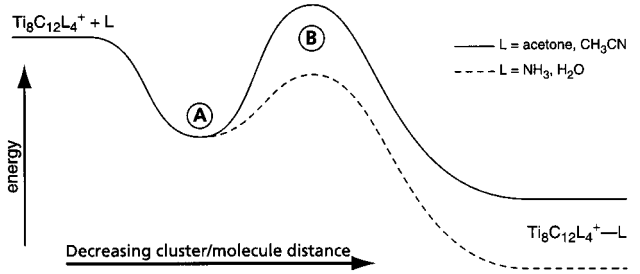

Figure 9. Qualitative potential energy surface showing the attachment of a fifth ligand of acetone or CH_3CN (solid line) and NH_3 or H_2O (dashed line).

Reactions with Nonpolar Molecules (C_6H_6 and C_2H_4). C_6H_6 and C_2H_4 are fundamentally different from the polar molecules described above. They are nonpolar and do not contain heteroatoms with lone pairs of electrons. Castleman and co-workers explained the addition of only four C_6H_6 molecules to the $Ti_8C_{12}^+$ cluster by invoking side-on bonding between two carbon atoms on C_6H_6 with two adjacent metal centers in the pentagonal rings of the T_h symmetry cluster.[12] Consequently, the addition of four C_6H_6 molecules ties up all eight metal atoms. This is an unusual bonding mode for C_6H_6 as the σ-bonding to the cluster would disrupt the aromaticity of C_6H_6. Alternatively, the addition of only four C_6H_6 molecules to the cluster can be explained by invoking the normal η^6-C_6H_6 coordination to a single metal atom. Such a coordination mode would only allow for the addition of four C_6H_6 molecules due to steric hindrance.

For a cluster with T_h symmetry, a C_6H_6 molecule would coordinate to a single metal atom through the π-system. The three metal centers directly adjacent to the coordinated metal are blocked from coordinating a C_6H_6 molecule due to steric factors. For the cluster with T_d symmetry, the C_6H_6 molecules would preferentially bind to the "outer" set of metal atoms with the "inner" set of metal atoms sterically blocked.

Due to the slow kinetics for addition of C_2H_4 to the cluster, we only were able to see the attachment of three molecules. However, Castleman and co-workers observed the addition of four C_2H_4 molecules with the addition clearly stopped at this point.[12] They suggested a similar bonding mode for C_2H_4 as for C_6H_6, with the C_2H_4 molecule bridging between two adjacent Ti atoms on a pentagonal ring. However, C_2H_4 may very well coordinate to a single Ti center according to the conventional Dewar−Chatt−Duncanson model. Again, in this bonding mode, a coordinated C_2H_4 would sterically hinder the three adjacent Ti metal atoms in the cluster with T_h symmetry. Consequently, only four C_2H_4 molecules can add to the cluster. For the cluster with T_d symmetry, only the "outer" set of metal atoms could coordinate C_2H_4. The slow kinetics for the addition of C_2H_4 to the cluster suggest a relatively weak interaction.

Conclusions

The results presented here show that the kinetics for attachment of small polar ligands to $Ti_8C_{12}^+$ varies with the number of attached ligands. This result is in contrast to the observations of Castleman and co-workers, where only rapid additions were observed.[1−5] Where the high-pressure reaction cell used in their experiments revealed the attachment of eight polar ligands at approximately the same rates, our lower pressure studies have shown that there is a dramatic change in the kinetics after the addition of the fourth ligand. We believe that the difference between the two groups is due to the reaction cell conditions. Castleman and co-workers carried out their reactions in a high-pressure ($\sim$0.7 Torr) reaction cell, whereas our reactions occur at a much lower pressure ($\sim 3 \times 10^{-6}$ Torr).

Small, polar molecules containing a heteroatom with a lone pair of electrons should interact with the positive titanium atoms largely by electrostatic attraction. The energy of this attraction should increase with polarity of the molecules. However, for the most polar molecules (CH_3CN and acetone), only four attachments are observed. For the less polar molecules (NH_3 and H_2O), the reaction efficiency decreases dramatically upon the addition of a fifth (NH_3) or sixth (H_2O) molecule. We explain these results by considering that the first four ligands coordinate to nonadjacent metal atoms, thereby minimizing repulsive forces between coordinated molecules. The fifth ligand must add to a metal atom where the three adjacent metal atoms are already coordinated. The strong repulsive forces upon approach of this fifth ligand would then reduce the reaction efficiency as observed. For the most polar molecules (CH_3CN and acetone), this repulsive force would be the greatest and can simply prevent further coordination.

For C_6H_6 and C_2H_4, the addition of only four ligands can be explained by simple π-coordination to a single metal center. The adjacent occupied metal atoms prevent further additions by simple steric hindrance.

A close examination of the ligand bonding properties of these metal−carbon cluster systems can lead us to a better understanding of their reactivities and kinetics, but gives little insight into their structural forms. The results presented here can be explained equally well in terms of either the T_h or T_d symmetry structures. It is possible that a theoretical study examining the rates of ligand addition to both the T_h and T_d structures could provide insight into the actual form of the cluster.

Acknowledgment. This paper is dedicated to the memory of Dr. Ben Sherman Freiser. Support for this research was provided by the National Science Foundation through Grant CHE-9627221.

References and Notes

(1) Guo, B. C.; Wei, S.; Purnell, J.; Buzza, S.; Castleman, A. W., Jr. *Science* **1992**, *256*, 515.
(2) Wei, S.; Guo, B. C.; Purnell, J.; Buzza, S.; Castleman, A. W., Jr. *Science* **1992**, *256*, 818.
(3) Guo, B. C.; Wei, S.; Chen, Z.; Kerns, K. P.; Purnell, J.; Buzza, S.; Castleman, A. W., Jr. *J. Chem. Phys.* **1992**, *97*, 5243.
(4) Wei, S.; Guo, B. C.; Purnell, J.; Buzza, S.; Castleman, A. W., Jr. *J. Chem. Phys.* **1992**, *96*, 4166.
(5) Guo, B. C.; Kerns, K. P.; Castleman, A. W., Jr. *J. Am. Chem. Soc.* **1993**, *115*, 7415.
(6) Pilgrim, J. S.; Duncan, M. A. *J. Am. Chem. Soc.* **1993**, *115*, 4395.
(7) Pilgrim, J. S.; Duncan, M. A. *J. Am. Chem. Soc.* **1993**, *115*, 6958.
(8) Yeh, C.-S.; Afzaal, S.; Byun, Y. G.; Freiser, B. S. *J. Am. Chem. Soc.* **1994**, *116*, 8806.
(9) Byun, Y. G.; Freiser, B. S. *J. Am. Chem. Soc.* **1996**, *118*, 3681.
(10) Byun, Y. G.; Lee, S. A.; Kan, S. Z.; Freiser, B. S. *J. Chem. Phys.* **1996**, *100*, 14281.
(11) Lee, S.; Gotts, N. G.; von Helden, G.; Bowers, M. T. *Science* **1995**, *267*, 999.
(12) Deng, H.-T.; Kerns, K. P.; Castleman, A. W., Jr. *J. Am. Chem. Soc.* **1996**, *118*, 446.
(13) Ceulemans, A.; Fowler, P. W. *J. Chem. Soc., Faraday Trans.* **1992**, *88*, 2797.
(14) Grimes, R. W.; Gale, J. D. *J. Chem. Soc., Chem. Commun.* 1992, 1222.
(15) Rohmer, M.-M.; de Vaal, P.; Bénard, M. *J. Am. Chem. Soc.* **1992**, *114*, 9696.
(16) Chen, H.; Feyereisen, M.; Long, X. P.; Fitzgerald, G. *Phys. Rev. Lett.* **1993**, *71*, 1732.
(17) Lin, Z.; Hall, M. B. *J. Am. Chem. Soc.* **1993**, *115*, 11165.
(18) Methfessel, M.; van Schilfgaarde, M.; Scheffler, M. *Phys. Rev. Lett.* **1993**, *71*, 209.
(19) Rohmer, M.-M.; Bénard, M.; Henriet, C.; Bo, C.; Poblet, J.-M. *J. Chem. Soc., Chem. Commun.* **1993**, 1182.
(20) Reddy, B. V.; Khanna, S. N. *J. Chem. Phys.* **1994**, *98*, 9446.
(21) Khan, A. J. *J. Chem. Phys.* **1995**, *99*, 4923.
(22) Rohmer, M.-M.; Bénard, M.; Bo, C.; Poblet, J.-M. *J. Am. Chem. Soc.* **1995**, *117*, 508.
(23) Dance, I. *J. Am. Chem. Soc.* **1996**, *118*, 6309.
(24) Pauling, L. *Proc. Natl. Acad. Sci. U.S.A.* **1992**, *89*, 8125.
(25) Cody, R. B.; Kissinger, J. A.; Ghaderi, S.; Amster, I. J.; McLafferty, F. W.; Brown, C. E. *Anal. Chim. Acta* **1985**, *178*, 43.
(26) Gord, J. R.; Freiser, B. S. *Anal. Chim. Acta* **1989**, *225*, 11.
(27) Maruyama, S.; Anderson, L. R.; Smalley, R. E. *Rev. Sci. Instrum.* **1990**, *61*, 3686.
(28) Chen, Z. Y.; Guo, B. C.; May, B. D.; cartier, S. F.; Castleman, A. W., Jr. *Chem. Phys. Lett.* **1992**, *198*, 118.
(29) Carlin, T. J.; Freiser, B. S. *Anal. Chem.* **1983**, *55*, 571.
(30) Bartmess, J. E.; Georgiadis, R. M. *Vacuum* **1983**, *33*, 149.
(31) Wang, T.-C. L.; Ricca, T. L.; Marshall, A. G. *Anal. Chem.* **1986**, *58*, 2935.
(32) Speir, J. P.; Gorman, G. S.; Pitsenberger, C. C.; Turner, C. A.; Wang, P. P.; Amster, I. J. *Anal. Chem.* **1993**, *65*, 1746.
(33) Hendrickson, C. L.; Drader, J. J.; Laude, D. A., Jr. *J. Am. Soc. Mass Spectrom.* **1995**, *6*, 448.
(34) Bruce, J. E.; Anderson, G. A.; Hofstadler, S. A.; Van Orden, S. L.; Sherman, M. S.; Rockwood, A. L.; Smith, R. D. *Rapid Commun. Mass Spectrom.* **1993**, *7*, 914.
(35) Su, T.; Bowers, M. T. *Int. J. Mass Spectrom. Ion Processes* **1973**, *12*, 247.
(36) Su, T.; Bowers, M. T. *Int. J. Mass Spectrom. Ion Processes* **1975**, *17*, 211.
(37) Woodin, R. L.; Beauchamp, J. L. *Chem. Phys.* **1979**, *41*, 1.
(38) Lide, D. R. *CRC Handbook of Chemistry and Physics*, 75th ed.; CRC Press: Boca Raton, FL, 1994.